RESEARCH ACTIVITIES VIII
Laser Research Center for Molecular Science

VIII-A Developments and Researches of New Laser Materials

Although development of lasers is remarkable, there are no lasers which lase in ultraviolet and far infrared regions. However, it is expected that these kinds of lasers break out a great revolution in not only the molecular science but also in the industrial world.

In this project we research characters of new materials for ultraviolet and far infrared lasers, and develop new lasers by using these laser materials.

VIII-A-1 Supercritical-Fluid Cell with Device of Variable Optical Path Length Giving Fringe-Free Terahertz Spectra

SAITOW, Ken-ichi[1]; NISHIKAWA, Keiko[1]; OHTAKE, Hideyuki; SARUKURA, Nobuhiko; MIYAGI, Hiroshi[2]; SHIMOKAWA, Yuji[2]; MATSUO, Hitoshi[3]; TOMINAGA, Keisuke[4]
([1]Chiba Univ.; [2]Gakushuin Univ.; [3]Matsuo Kogyosho, Inc.; [4]Kobe Univ.)

[*Rev. Sci. Instrum.* **71**, 4061 (2000)]

An optical cell suitable for supercritical fluids was constructed for measurements of far infrared absorption spectra with terahertz radiation as a light source. It was designed to withstand temperature up to 400 K and pressure up to 15 MPa. The cell has two characteristic devices; one is diamond windows set in the Brewster angle to the incident far infrared light and the other is a variable optical path length from 30 μm to 20 mm under high pressure conditions. Using the cell, fringe-free spectra of CHF_3 ranging from low-density gaseous states to high-density supercritical ones were measured in a low-energy region of 10–100 cm^{-1}.

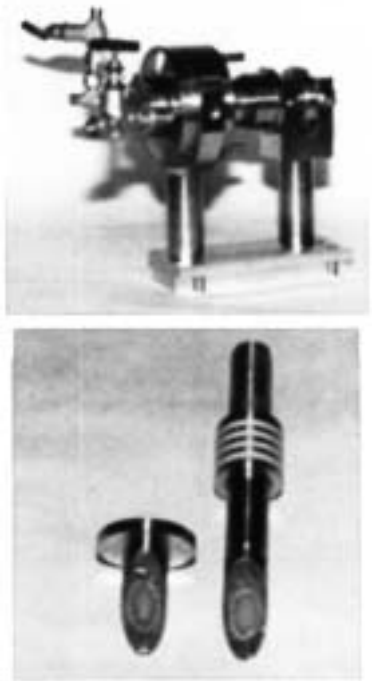

Figure 1. Photographs of an optical cell for far infrared absorption spectra measurements of supercritical fluids. The cell itself is shown in the upper part. The lower part represents flanges with diamond windows set in the Brewster angle, a cylinder, and a V packing.

VIII-A-2 Growth and Characterization of $KMgF_3$ Single Crystals by the Czochralski Technique under CF_4 Atmosphere

SHIMAMURA, Kiyoshi[1]; FUJITA, Tomoyo[1]; SATO, Hiroki[1]; BENSALAH, Amina[1]; SARUKURA, Nobuhiko; FUKUDA, Tsuguo[1]
([1]Tohoku Univ.)

[*Jpn. J. Appl. Phys., Part 1* **39**, 6807 (2000)]

$KMgF_3$ (KMF) single crystals were grown by the Czochralski technique as a new candidate of vacuum-ultra-violet optical materials. The absorption edge of KMF single crystals was 115 nm. The distribution of birefringence in the radial direction was of the order of 10^{-7}. The thermal expansion coefficient of KMF single crystals along the <111> orientation was 1.98×10^{-5} K^{-1}. Together with its excellent mechanical properties, these characteristics show KMF to be superior to the current materials.

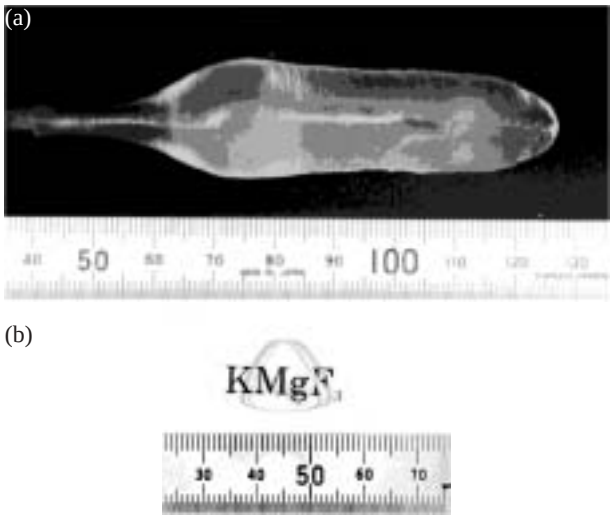

Figure 1. (a) As-grown $KMgF_3$ single crystal of 20 mm diameter pulled along the <111> orientation and (b) $KMgF_3$-wafer cut perpendicular to the growth axis with thickness of 2 mm.

VIII-A-3 Chirped-Pulse Amplification of Ultraviolet Femtosecond Pulses by Use of Ce^{3+}:$LiCaAlF_6$ as a Broadband, Solid-State Gain Medium

LIU, Zhenlin[1]; KOZEKI, Toshimasa; SUZUKI, Yuji; SARUKURA, Nobuhiko; SHIMAMURA, Kiyoshi[2]; FUKUDA, Tsuguo[2]; HIRANO, Masahiro[1]; HOSONO, Hideo[1,3]
([1]ERATO; [2]Tohoku Univ.; [3]Tokyo Inst. Tech.)

[*Opt. Lett.* **26**, 301 (2001)]

Chirped-pulse amplification in the ultraviolet region is demonstrated by use of a broadband Ce^{3+}:$LiCaAlF_6$ laser medium. A modified bow-tie-style four-pass amplifier pumped by 100-mJ, 266-nm pulses from a *Q*-switched Nd:YAG laser has a gain factor of 370 and delivers 6-mJ, 290-nm pulses. After dispersion compensation, the output pulses can be compressed to 115 fs.

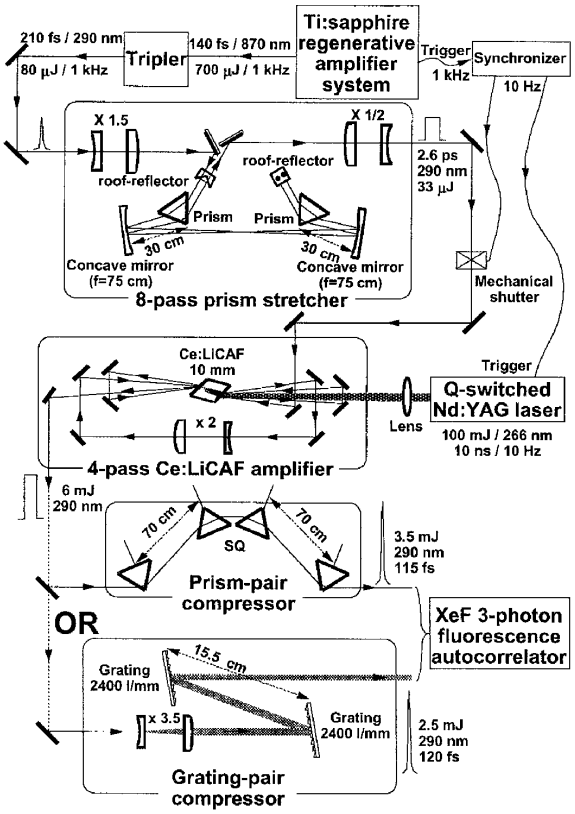

Figure 1. Experimental setup of the Ce:LiCAF CPA laser system. SQ, synthetic quartz.

VIII-A-4 Terahertz Radiation from a Shallow Incidence-Angle InAs Emitter in a Magnetic Field Irradiated with Femtosecond Laser Pulses

ONO, Shingo[1]; TSUKAMOTO, Takeyo[1]; KAWAHATA, Eiji; YANO, Takayuki; OHTAKE, Hideyuki; SARUKURA, Nobuhiko
([1]Sci. Univ. Tokyo)

[*Appl. Opt.* **40**, 1369 (2001)]

The optimized incidence angle and magnetic field direction geometry of an InAs terahertz radiation emitter irradiated with femtosecond laser pulses in a magnetic field is reported. The optimum geometric layout is the magnetic field direction parallel to the semiconductor surface and at an incidence angle that is slightly larger than the Brewster angle. Additionally, we also observed a center frequency shift of terahertz radiation spectrum by changing the incidence angle of the excitation laser.

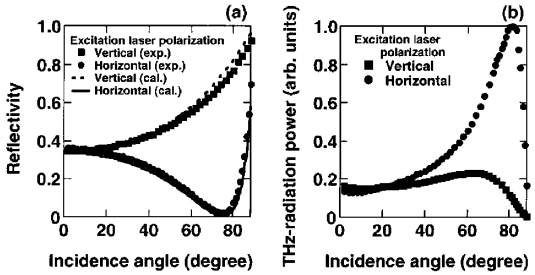

Figure 1. Angular dependence of (a) 800-nm excitation laser reflectivity and (b) THz radiation intensity from InAs. The solid and dotted curves represent the results of our theoretical calculations for $n = 3.729$ and $k = 0.448$.

VIII-A-5 Crystal Growth of Ce-Doped and Undoped $LiCaAlF_6$ by the Czochralski Technique under CF_4 Atmosphere

SHIMAMURA, Kiyoshi[1]; BALDOCHI, Sonia L.[1]; RANIERI, Izilda M.[1]; SATO, Hiroki[1]; FUJITA, Tomoyo[1]; MAZZOCCHI, Vera L.[2]; PARENTE, Carlos B. R.[2]; PAIVA-SANTOS, Carlos O.[3]; SANTILLI, Celso V.[3]; SARUKURA, Nobuhiko; FUKUDA, Tsuguo[1]
([1]Tohoku Univ.; [2]Nucleares-IPEN/CNEN-SP; [3]UNESP)

[*J. Cryst. Growth* **223**, 382 (2001)]

Ce-doped and undoped $LiCaAlF_6$ (LiCAF) single crystals 50 mm in diameter were grown by the Czochralski technique. The formation of inclusions and cracks accompanying the crystal growth was investigated. The dependence of lattice parameters on the temperature was measured for LiCAF and $LiSrAlF_6$ single crystals. Linear thermal expansion coefficients for both these crystals were evaluated. Higher transmission properties for LiCAF single crystals were achieved in the UV and VUV wavelength regions.

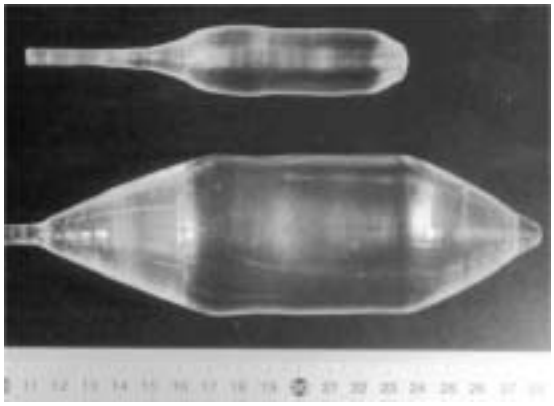

Figure 1. As-grown 2" diameter Ce-doped $LiCaAlF_6$ single crystal.

VIII-A-6 Ultraviolet Femtosecond Pulse Amplification with High Gain Using Solid-State, Broad-Band Gain Medium Ce^{3+}:$LiCaAlF_6$

LIU, Zhenlin[1]; KOZEKI, Toshimasa; SUZUKI, Yuji; SARUKURA, Nobuhiko; SHIMAMURA, Kiyoshi[2]; FUKUDA, Tsuguo[2]; HIRANO, Masahiro[1]; HOSONO, Hideo[1,3]
([1]ERATO; [2]Tohoku Univ.; [3]Tokyo Inst. Tech.)

[*Jpn. J. Appl. Phys., Part 1* **40**, 2308 (2001)]

Femtosecond pulse amplification with high gain in the ultraviolet region has been demonstrated using the solid-state, broad-band crystal Ce^{3+}:$LiCaAlF_6$. With the seed pulses coming from the third harmonic generation of a cw mode-locked Ti:sapphire laser, the confocal, four-pass amplifier pumped by 15-mJ, 266-nm, 10-ns pulses from a Q-switched Nd:YAG laser demonstrates 60-dB gain and delivers 54-μJ, 289-nm, 200-fs, 10-Hz pulses. There is almost no satellite pulse even without any special single-pulse selection.

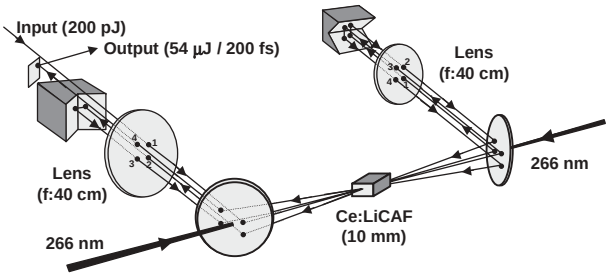

Figure 1. Experimental setup of the confocal, four-pass Ce:LiCAF amplifier. The input is the frequency-tripled output of a cw mode-locked femtosecond Ti:sapphire laser.

VIII-A-7 Terahertz Absorption Spectra of Supercritical CHF_3 to Investigate Local Structure Through Rotational and Hindered Rotational Motions

SAITOW, Ken-ichi[1]; OHTAKE, Hideyuki; SARUKURA, Nobuhiko; NISHIKAWA, Keiko[1]
([1]Chiba Univ.)

[*Chem. Phys. Lett.* **341**, 86 (2001)]

Far infrared absorption spectra of neat supercritical fluoroform (CHF_3) are measured with terahertz (THz) radiation. The spectra covering from 10 to 100 cm^{-1} are obtained at reduced temperature $T/T_c = 1.02$ on densities varied by a factor of 200. As density increases, dominant component of spectra changes from rotational to hindered-rotational motion. However, the change is nonlinear to the density. Such specificity arises from difference between bulk and local densities, and the most enhanced local density is observed near the thermodynamic state of maximum density fluctuation. In the pure fluid system, the relationship between density fluctuation and local density enhancement is experimentally presented.

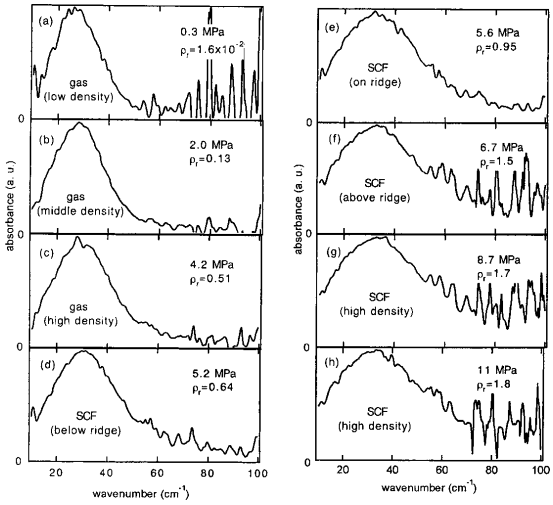

Figure 1. Far infrared absorption spectra of supercritical CHF_3 measured at reduced temperature by $T_r = T/T_c = 1.02$. The (a)–(c) are data below critical pressure (P_c) and (d)–(h) those of above P_c. The (d), (e), and (f) are ones below, on, and above the ridge, respectively. The (g) and (h) are ones at dense supercritical states above the ridge.

VIII-A-8 Observation of New Excitation Channel of Ceriumion through Highly Vacuumultraviolet Transparent LiCAF Host Crystal

KOZEKI, Toshimasa; SUZUKI, Yuji; SAKAI, Masahiro; OHTAKE, Hideyuki; SARUKURA, Nobuhiko; LIU, Zhenlin; SHIMAMURA, Kiyoshi[1]; NAKANO, Kenji; FUKUDA, Tsuguo[1]
([1]Tohoku Univ.)

[*J. Cryst. Growth* **229**, 501 (2001)]

The transmission spectra of $LiCaAlF_6$ (LiCAF) and $LiSrAlF_6$ (LiSAF) are investigated in the ultraviolet (UV) and the vacuum ultraviolet (VUV) region. The transmission edge of LiCAF (112 nm) shows almost the same value as that of LiF. Taking into account difficulties of material processing and polishing due to the cleavage or the hydroscopic nature of LiF, LiCAF is regarded as a more suitable optical material in the UV and the VUV region. Moreover, the new excitation channel around 112 nm is discovered for Ce:LiCAF crystal. This excitation is originated not from absorption of Ceriumions but fromabsorption around the bandgap of the host crystal.

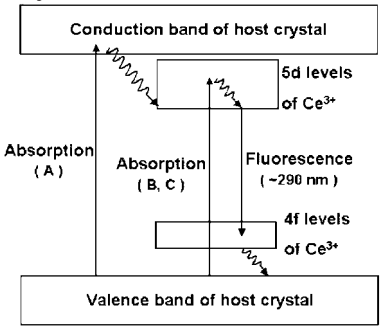

Figure 1. Schematic of energy levels and possible decay channel in Ce:LiCAF crystal.

VIII-A-9 THz-Radiation Emitter and Receiver System Based on a 2 T Permanent Magnet, 1040 nm Compact Fiber Laser and Pyroelectric Thermal Receiver

OHTAKE, Hideyuki; SUZUKI, Yuji; SARUKURA, Nobuhiko; ONO, Shingo[1]; TSUKAMOTO, Takeyo[1]; NAKANISHI, Akio[2]; NISHIZAWA, Seiji[3]; STOCK, Michelle L.[4]; YOSHIDA, Makoto[4]; ENDERT, Heirich[4]

([1]Sci. Univ. Tokyo; [2]Sumitomo Special Metal Co., Ltd.; [3]Shinshu Univ.; [4]Imra America, Inc.)

[*Jpn. J. Appl. Phys.* in press]

Thermal receiver detectable terahertz (THz) radiation is generated from InAs irradiated with a 1040 nm, 80 fs, 180 mW, 48-MHz-repetition-rate mode-locked fiber laser in a 2 T field by a compact permanent magnet. THz radiation is monitored by means of a deuterated triglycine sulfate (DTGS) pyroelectric thermal receiver. DTGS operates at room temperature and does not require time-gating adjustment or cryogen cooling with liquid helium. The THz-radiation emitter system, including the excitation laser head, is almost the same size as a conventional notebook computer.

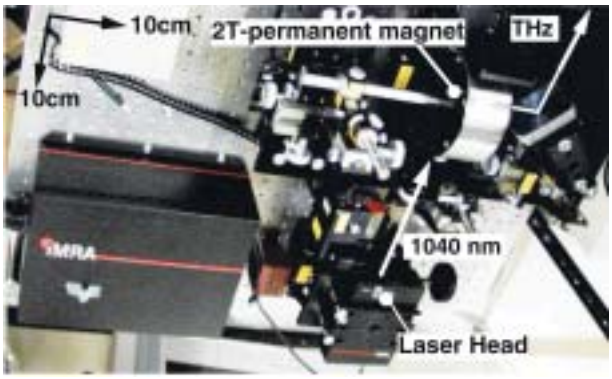

Figure 1. Photograph of THz-radiation emitter system. Laser beam is focused onto the sample with a 2 T permanent magnet.

VIII-A-10 Nanocluster Crystals of Lacunary Polyoxometalates as Structure-Design-Flexible, Inorganic Nonlinear Materials

MURAKAMI, Hidetoshi; KOZEKI, Toshimasa; SUZUKI, Yuji; ONO, Shingo[1]; OHTAKE, Hideyuki; SARUKURA, Nobuhiko; ISHIKAWA, Eri[2]; YAMASE, Toshihiro[2]

([1]Sci. Univ. Tokyo; [2]Tokyo Inst. Tech.)

[*Appl. Phys. Lett.* in press]

Lacunary polyoxometalates, large inorganic, structure-design-flexible, nanocluster crystals are found to have higher optical nonlinearity than KH_2PO_4 (KDP) by the powder second-harmonic-generation (SHG) method. Moreover, the capability of generating ultra-violet radiation down to around 300 nm is found. The basic criteria to design the high nonlinearity are also discovered by the reduction of the molecular symmetry.

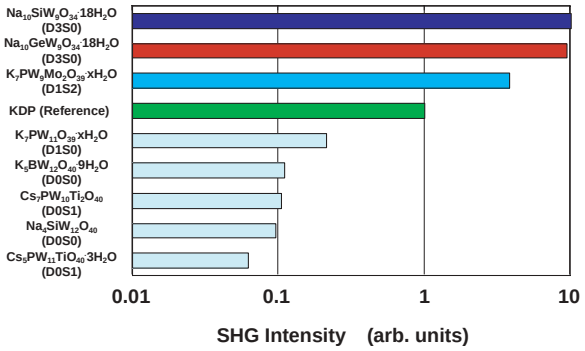

Figure 1. Powder second-harmonic-generation method results using a 1064-nm optical pulse from a Q-switched Nd:YAG laser as the fundamental radiation. Label S denotes the substitution number of metal atom.

VIII-B Development and Research of Advanced Tunable Solid State Lasers

Diode-pumped solid-state lasers can provide excellent spatial mode quality and narrow linewidths. The high spectral power brightness of these lasers has allowed high efficiency frequency extension by nonlinear frequency conversion. Moreover, the availability of new and improved nonlinear optical crystals makes these techniques more practical. Additionally, quasi phase matching (QPM) is a new technique instead of conventional birefringent phase matching for compensating phase velocity dispersion in frequency conversion. These kinds of advanced tunable solid-state light sources, so to speak "Chroma Chip Lasers", will assist the research of molecular science.

In this projects we are developing Chroma Chip Lasers based on diode-pumped-microchip-solid-sate lasers and advanced nonlinear frequency conversion technique.

VIII-B-1 Intra-Cavity Frequency Doubling of a Nd:YAG Laser Passively Q-Switched by Cr^{4+}:YAG Saturable Absorber

PAVEL, Nicolaie; SAIKAWA, Jiro; KURIMURA, Sunao; TAIRA, Takunori

[*Conf. Lasers Electro-Opt.* CTuM27 (2001)]

Frequency doubling of a diode-pumped, passively Q-switched laser could be a convenient method of generating pulsed laser sources in green region. The external-cavity frequency doubling simplifies the cavity design and the green pulses are shorter than that of the Q-switched laser. However, this method is applicable to laser sources that operate with high output powers,[1] such that acceptable conversion efficiencies can be realized. On the other hand, intra-cavity frequency doubling made uses of the high peak power that is present inside the cavity, therefore resulting in higher conversion efficiency. A disadvantage of this scheme could be the longer pulses than those produced by a comparable Q-switched laser with no intra-cavity doubling. However, if the accurate pulse width is not critical for application such pulses would reduce the possibility of various types of optical damages. In this work we report a diode-pumped Nd:YAG laser passively Q-switched by a Cr^{4+}:YAG saturable absorber (SA) and intra-cavity frequency doubled by a LBO crystal. The maximum green average power was ~1.0 W, with the laser operating at 3.8 kHz repetition frequency and 87.8-ns pulses duration (263 μJ pulse energy, ~3 kW peak power).

Figure 1 shows a schematic layout of the laser. As pump source we used a 1.55-mm diameter, 0.11 NA fiber-bundled diode (OPC-B030-mmm-FC, OptoPower Co.). We considered a Nd:YAG medium (6-mm diameter, 10-mm length, 1.3-at.%), AR coated at 808 nm on both sides. The plane mirror M1, which was coated for high reflection (HR) at 1.064 mm and high transmission (HT) at 808 nm, was used as the rear mirror of the resonator. The performances of the laser under continuous-wave (CW) operation were first investigated in a plane-plane resonator of 40-mm length. With a flat output mirror of 5% transmission at 1.064 mm we obtained a maximum output power of 8.9 W for an absorbed pump power of 21.0 W, in a laser beam with the M^2 factor of 2.2. The slope efficiency was 48.8%. The performances of the V-type cavity were next determined in CW operation. The plane mirror M^2 was HR coated at 1.064 μm and HT coated at 532 nm. The distances between mirrors M1 and M2, and M2 and M3 were 80 mm and 90 mm, respectively. With a mirror M3 of 50-cm radius and coated as 95% reflectivity at 1.064 μm, a maximum polarized infrared power of 3.8 W for 18.6 W absorbed pump power resulted. The laser beam M^2 factor was 1.14. A 3×3×10 mm^3 LBO crystal was considered for intra-cavity frequency doubling. It was designed for type I second-harmonic generation (critical phase-matching condition), therefore operating at the room temperature. Now M3 was a concave mirror of 50-cm radius and HR coated at both 1.064 mm and 532 nm wavelengths. Thus, 3.2 W green radiation for 18.6 W absorbed pump power in a beam of $M^2 = 1.5$ resulted.

Figure 2 summarize the output properties of the diode-pumped Nd:YAG laser, passively Q-switched by Cr^{4+}:YAG SA and intra-cavity frequency-doubled by LBO. Cr^{4+}:YAG SA crystals with unsaturated transmission T_0 of 90% and 80%, and that were AR coated at 1.064 mm were used. For the SA crystal of 90% initial transmission we obtained an average green power of 1.0 W for the absorbed pump-power of 14.1 W. The laser beam M^2 factor was 1.6. At this pump level the pulse width and the pulse repetition rate were 87.8 ns and 3.8 kHz and the corresponding pulse energy and peak power were 263 μJ and ~3.0 kW. A slightly higher peak power, namely 4.2 kW resulted for the SA of 80% initial transmission: the green average power was ~0.7 W and the pulse width and energy were 50 ns and 209 mJ, respectively. For comparative data on the Cr^{4+}:YAG crystal of 90% initial transmission, the LBO crystal was removed from the resonator and the mirror M3 was replaced by a 90% reflectivity mirror at 1.064 μm. Thus, an infrared maximum average power of 1.1 W resulted at 3.9 kHz and with pulses of 41.5 ns (pulse energy and the peak power were 282 mJ and ~6.8 kW, respectively). As expected, the green pulses were longer than those produced by a comparable Q-switched laser with no intra-cavity doubling. In order to explain the Q-switching results a rate-equation model that accounts for thermally induced effects in Nd:YAG rod, the ratio of the laser-beam area in medium gain to that in SA and its influence on Q-switch performances, and the SA exited state absorption (ESA) contribution was developed. The frequency doubling process was taken into account by introducing a nonlinear loss term in the flux equation rate.[2] Following the laser dynamics we have derived

analytical expressions that describes the Q-switched pulse energy, peak power, pulse width and repetition rate.[3] Using this model a good agreement between the experimental data and theory was obtained for both infrared and second-harmonic regimes.

In summary, we have reported a diode-pumped Nd:YAG laser, passively Q-switched by Cr^{4+}:YAG saturable absorber and intra-cavity frequency-doubled by LBO crystal. The laser produces high beam-quality of 263-μJ energy, 87.8-ns pulses at a pulse repetition rate of 3.8 kHz, for an average power of 1.0 W at 532 nm.

References

1) A. Agnesi, S. Dell'Acqua, E. Piccinini, G. Reali and G. Piccinno, *IEEE J. Quantum Electron.* **34**, 1480 (1998).
2) E.C. Honea, C.A. Ebbers, R. J. Beach, J. A. Speth, J. A. Skidmore, M. A. Emanuel and S.A. Payne, *Opt. Lett.* **23**, 1203 (1998).
3) N. Pavel, J. Saikawa, S. Kurimura, I. Shoji and T. Taira, *Technical Report of Japan Inst. for Electronics, Information and Commun. Engineers (IEICE)* **LQE-65**, 23 (2000).

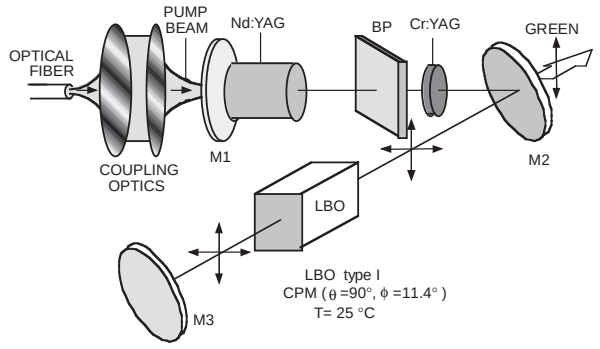

Figure 1. Schematics of the diode end-pumped Nd:YAG laser, passively Q-switched by Cr^{4+}:YAG SA and intra-cavity frequency-doubled by LBO crystal. BP: glass-plate positioned at the Brewster angle.

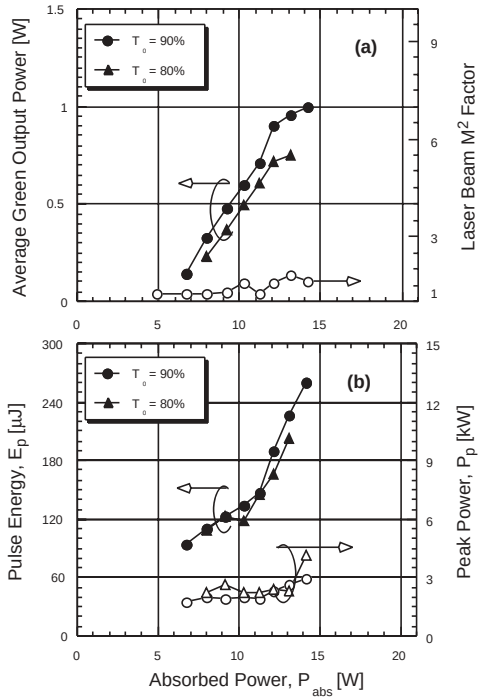

Figure 2. Output properties of diode-pumped Nd:YAG laser, passively Q-switched by Cr^{4+}:YAG and intra-cavity frequency-doubled by LBO. (a) Average power and laser-beam M^2 factor; (b) Pulse energy and pulse peak power.

VIII-B-2 Laser Emission under Resonant Pump in the Emitting Level of Highly Doped Nd Materials

LUPEI, Voicu[1]; TAIRA, Takunori; PAVEL, Nicolaie; SHOJI, Ichiro; IKESUE, Akio[2]
([1]IAP, Romania; [2]JFCC)

[*Conf. Lasers Electro-Opt.* CFD4 (2001)]

Heating effects in the laser active media under pump constitute a major limitation in the construction of highly efficient or high-power solid state lasers. These effects could induce the optical distortion of the resonator or even the physical destruction of the active component. In case of neodymium-doped crystals two major sources exists: the quantum defect between the pump and laser radiation and the non-radiative processes (multiphonon relaxation, down-conversion cross-relaxation on intermediate levels, upconversion from the emitting level $^4F_{3/2}$). While the non-radiative processes constitute a physically inherent loss, the quantum defect can be controlled by the pump and emission wavelengths. In the actual diode pumped Nd laser the pump is accomplished in the $^4F_{5/2}$ level (808.7 nm) and the excitation relaxes by electron-phonon interaction to the components R_1 and R_2 of the emitting level, placed at ~945 and 860 cm^{-1} below the pump level. In absence of laser emission about 39% from the absorbed pump radiation in $^4F_{5/2}$ is transformed into heat in a 1.04 at.% Nd:YAG crystal,[1] in accord with a theoretical modeling that accounts for the non-radiative effects on the quantum efficiency.[2] In case of an efficient laser emission, when the effect of the non-radiative processes is very small and the heat generation is dominated by the quantum defect the fractional thermal load in this sample is reduced up to about 0.25. However, this figure is much larger than the value of about 0.09 in case of Yb lasers, where the pump is performed in an upper crystal field component of the emitting level.

Pumping in the emitting level or even below it could be a very efficient means for reducing the heating effects in Nd lasers. Thus, in case of Nd:YAG laser, the pump can be performed in the lower component R_1 (11425.5 cm^{-1}) of $^4F_{3/2}$ and the population of the emitting level R_2 (11509 cm^{-1}) can be accomplished by thermal population (at the room temperature about 40% of the population of $^4F_{3/2}$ level is in the R_2 level). The thermallization of the energy levels can be also used for the reduction of the lower quantum defect, between the terminal and the ground level, by pumping in a hot band of the $^4I_{9/2} \rightarrow {}^4F_{3/2}$ absorption. The spectroscopic investigation of various Nd-doped crystals shows that there are many cases when the optical transitions $X_2 \rightarrow R_1$ and $X_3 \rightarrow R_2$ are very close or nearly degenerate, leading to a two- or single-peaked broad feature: at room temperature the population of crystal field components X_2 and X_3 of $^4I_{9/2}$ could be large (in YAG

these are 0.246 and 0.178, respectively), leading to a very fairly good absorption of pump. Using these effects (thermal population—assisted pump) is equivalent with a photon cooling. However, since the quantum defect is still positive this is not evidenced as a net cooling of the same sample but only as a reduction of the thermal load. It must be noted that the attempt to observe the laser cooling in Nd:YAG[3] used the pump with 1.06 micron wavelength in order to excite the tiny fraction of thermal population from the $^4I_{11/2}$ level up to the emitting level $^4F_{3/2}$.

The room temperature absorption spectra of Nd:YAG show these two transitions collected in a two-peaked (885.7 nm and 884.4 nm) broad feature centred around 885 nm. For 1 at.% Nd the absorption coefficient for the two peaks is almost equal, ~1.75 cm^{-1}, *i.e.* much weaker than the 808.7 nm pump transition (~ 9 cm^{-1}). Laser emission has been demonstrated for 1 at.% Nd:YAG crystal[4] under 885 nm pump. However, the weak absorption of this radiation in the crystal samples precludes the construction of either microchip or high-power lasers.

Recent studies revealed that highly doped Nd:YAG laser components can be fabricated by ceramics technique.[5,6] The spectroscopic investigation shows that the intensity of the 885 nm band increases linearly with the Nd concentration, the two peaks reaching an absorption coefficient of over 14 cm^{-1} for the 9 at.% sample (Figure 1). At the same time the width of the absorption feature increases by about 25%, from 2.5 nm FWHH to 3.15 nm, by increasing the Nd concentration from 1 to 9 at.%.

In case of Nd:YAG the fractional thermal load is expected to reduce to 0.318 for 1 at.% and to 0.66 for 3.4 at.% Nd under 885 nm pump in absence of laser emission. The most important reduction will be in presence of laser emission, to 0.168 for 1.06 mm emission, *i.e.* a reduction of over 40% from the case with 808 nm pump, and to 0.058 for 940 nm emission, lower than for Yb:YAG laser and with a terminal level (852 cm^{-1}) higher than that of Yb (612 cm^{-1}).

The continuous-wave laser emission in highly doped Nd:YAG ceramics under 885 nm pump was tested with an uncoated active component of 3.4 at.% Nd and 0.87 mm thickness (Figure 2). This was placed in a 25-mm plane-concave resonator with a 50-mm radius output mirror. The 885 nm pump was provided by a Ti:sapphire laser, whose radiation was focussed to a 80 μm diameter in the active medium. For a 95% output mirror reflectivity the laser delivered 42 mW at 1.064 μm for an absorbed pump power of 194 mW; the threshold pump power and the slope efficiency were 87 mW and 37.5%, respectively. With an output mirror reflectivity of 99% the pump threshold dropped to 38 mW but the slope efficiency decreased at 16.7%, while the maximum output power was 27 mW with an optical efficiency of 14%. The improvement of laser performances is under study, by considering coated Nd:YAG ceramic components of optimized size, an improved configuration for the laser resonator as well as an increased pump power.

In conclusion this study shows that the highly doped Nd:YAG ceramics as well as many crystals with high concentrations of Nd ions could be systems of choice for low heat – high power or miniature lasers with hot band (885 nm in case of Nd:YAG) resonant pump.

References

1) T. Y. Fan, *IEEE J. Quantum Electron.* **29**, 1457 (1993).
2) V. Lupei and A. Lupei, *Phys. Rev. B* **61**, 8087 (2000).
3) T. Kushida and J. E. Geusic, *Phys. Rev. Lett.* **21**, 1172, (1968).
4) R. Lavi and S. Jackel, *Appl. Opt.* **39**, 3093 (2000).
5) I. Shoji, S. Kurimura, Y. Sato, T. Taira, A. Ikesue, and K. Yoshida, *Appl. Phys. Lett.* **77**, 939 (2000).
6) J. Lu, M. Prabhu, J. Song, C. Li, J. Xu, K. Ueda, A. A. Kaminskii, H Yagi and T. Yanagitani, *Appl. Phys. B: Lasers Opt.* **71**, 46 (2000).

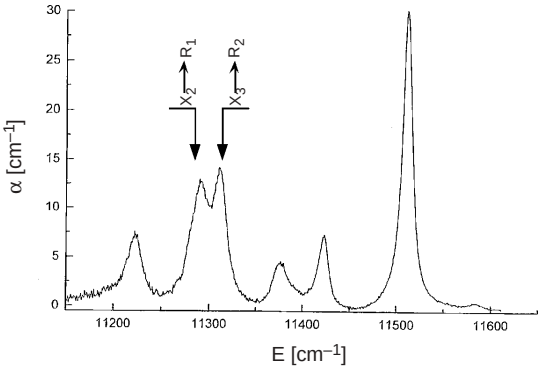

Figure 1. Room temperature $^4I_{9/2} \rightarrow {}^4F_{3/2}$ absorption spectrum of the 9 at.% Nd:YAG ceramics.

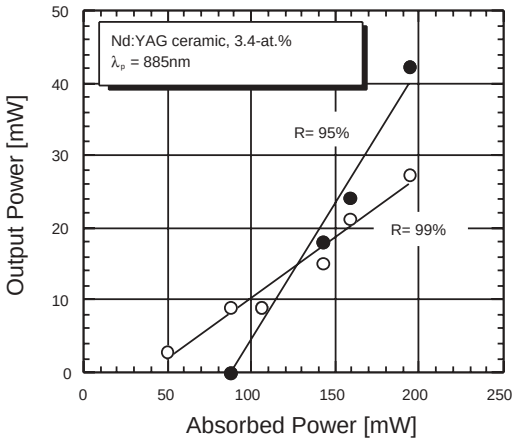

Figure 2. Output to input characteristics for the uncoated 3.4-at.% Nd:YAG ceramic pumped at 885 nm.

VIII-B-3 Thermal Birefringence in Nd:YAG Ceramics

SHOJI, Ichiro; SATO, Yoichi; KURIMURA, Sunao; LUPEI, Voicu; TAIRA, Takunori; IKESUE, Akio[1]; YOSHIDA, Kunio[2]
([1]JFCC; [2]Osaka Inst. Tech.)

[*Conf. Lasers Electro-Opt.* CFD6 (2001)]

Nd:YAG ceramics are promising candidates for high-power and high-efficiency microchip laser materials because highly transparent and highly Nd^{3+}-doped samples are available without degrading thermo-mechanical properties; the thermal conductivity is as

high as that of single-crystal YAG even at high Nd^{3+} concentrations. We have succeeded in microchip laser oscillation, in which the output power from a microchip of a 3.4 at. % Nd:YAG ceramic was more than twice as high as that from a same sized microchip of a Nd:YAG single crystal at the same input power. In this work we have investigated thermal birefringence effect in the Nd:YAG ceramics, which should be useful for power scaling.

Thermal birefringence of Nd:YAG ceramics was measured with the pump-probe experiment. A Ti:sapphire laser oscillating at 808 nm was used as the pump beam. The pump beam was focused onto the sample with the radius of 80 μm. On the other hand, linearly polarized He-Ne laser beam was used as the probe beam, and only the depolarized component of the probe beam was detected by use of a polarizer. If the depolarization is defined by the ratio of the depolarized power to the total probe power, dependence of the depolarization on the absorbed pump power for the ceramic and single-crystal samples with various Nd^{3+} concentrations is shown in Figure 1. On the other hand, Figure 2 shows the depolarization as a function of Nd^{3+} concentration at the absorbed pump power of 1000 mW. We found that the depolarization is nearly the same between the ceramic and single-crystal YAG if they have equal Nd^{3+} concentrations. This result indicates that the average of the thermal birefringence induced in the Nd:YAG ceramics is nearly the same with that in the (111)-cut single crystal. Moreover, it was also found that the depolarization became larger in samples with higher Nd^{3+} concentrations even if the same pump power was absorbed. This is mainly attributed to the fact that the fractional thermal loading increases as Nd^{3+} concentration becomes higher. When lasing occurs, on the other hand, thermal birefringence is expected to be greatly reduced because the thermal loading is then independent of Nd^{3+} concentration.

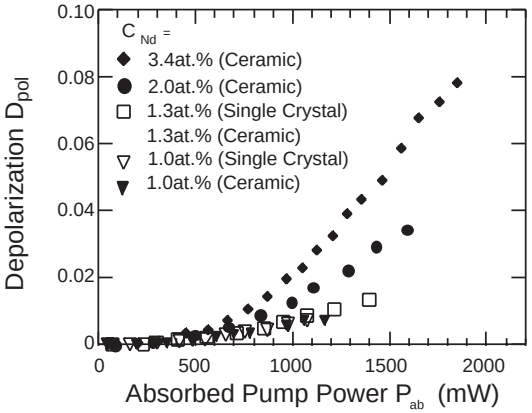

Figure 1. Dependence of the depolarization on the absorbed pump power for the ceramic and single-crystal samples with various Nd^{3+} concentrations.

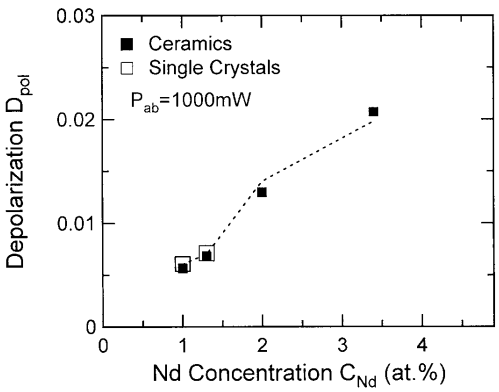

Figure 2. Depolarization as a function of the Nd^{3+} concentration for the ceramic and single-crystal samples at the absorbed pump power of 1000 mW. The dotted curve is the calculated result.

VIII-B-4 In-situ Observation of Fabrication of Nonlinear Optical Wavelength Converter

KURIMURA, Sunao; SHOJI, Ichiro; TAIRA, Takunori; RO, Jung Hoon[1]; CHA, Myoungsi[1]
([1]Pusan Natl. Univ.)

[*Conf. Lasers Electro-Opt.* 3a-Q-22(2001)]

MgO-doped $LiNbO_3$ (MgO:LN) has attracted much attention in quasi-phase-matched (QPM) wavelength conversion due to high resistance to photorefractive damage and low coercive field allowing a large aperture device. Since our first measurement of the coercive field, the crystal has become popular in QPM application and recent works have been verifying high performance of the material. To improve device characteristics, characterization of the domain movement is required for a device with larger aperture. Here we report in-situ monitored poling process and coercive field depending on Mg content in MgO:LN.

The experimental setup for poling is illustrated in Figure 1(a). We used transparent liquid electrode system consisting of transparent plastic blocks and o-rings. Z-cut MgO:LN wafers were sandwiched between two o-rings filled with LiCl electrodes. We observed ferroelectric 180° domains by the electro-optic imaging (EOI) technique under the crossed polarizers. Although EOI technique has a moderate spatial resolution compared with other techniques such as second-harmonic-generation microscope we previously developed, it allows in-situ observation of the poling process with a simple setup. Owing to the small velocity of domain wall in MgO:LN, real-time development was recorded by a commercial video camera. Figure 1(b) shows selected pictures describing the wall movement. Domains with reversed polarization nucleated from the right top corner in the square area directly exposed to the liquid electrode on the +C face. Walls creep very slowly and monitored current has Barkhausen pulses as we reported before. Observed bright spots work as traps of walls, making Barkhausen pulses in current.

We measured coercive fields (Ec) for forward and backward poling in 1mm-thick various crystals with different Mg concentrations of 1–7 mol%. Figure 1(c)

presents a significant reduction of coercive field with high doping of Mg. For forward poling, first polarization reversal in fresh wafers, Ec has a minimum value of 4.6 kV/mm at 5 mol%. This corresponds to the lowest defect density at this doping level in the crystal. On the other hand, for backward poling, first polarization reversal after forward poling, Ec decreases monotonically up to 7 mol%. The minimum value we observed here is 2.3 kV/mm at 7 mol%.

In conclusion, we report coercive field dependence on Mg content in LN crystals while observing polarization reversal process simultaneously with poling. Forward coercive field exhibits the minimum value of 4.6 kV/mm at 5 mol% and backward coercive field has the lowest value of 2.3 kV/mm at highest doping level of 7 mol%.

(a)

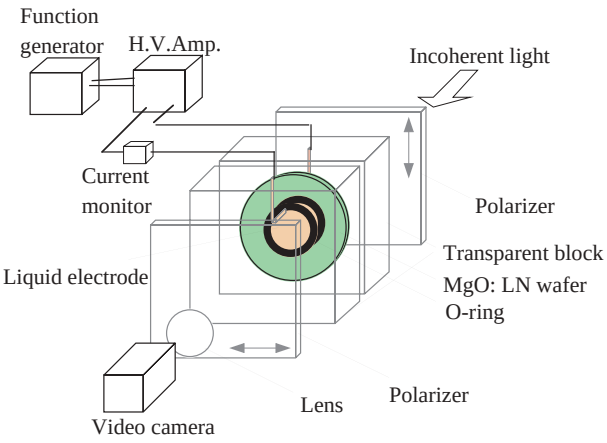

(b)

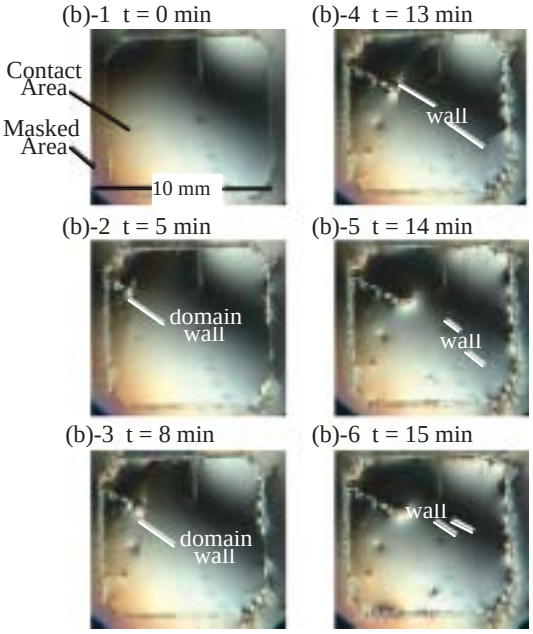

(c)

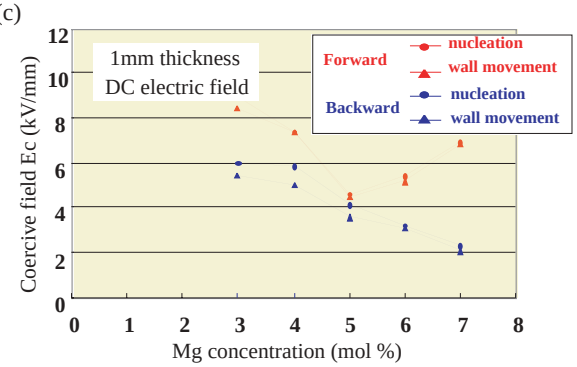

Figure 1. (a) Experimental setup of *in-situ* observation of poling process (b) time development of domains in MgO:LN during electric field poling process (c) coercive field dependence on Mg concentration in MgO:LN.

VIII-B-5 Periodical Twinning in Crystal Quartz for Ultraviolet Nonlinear Optics

KURIMURA, Sunao; FEJER, Martin[1]; SHOJI, Ichiro; TAIRA, Takunori; UESU, Yoshiaki[2]; NAKAJIMA, Hirochika[2]
([1]Stanford Univ., USA; [2]Waseda Univ.)

[*Oyobuturi* **69**, 548 (2000)]

Crystal quartz has low absorption, high chemical stability, and low thermooptic coefficients, attractive for operation in ultraviolet nonlinear optics. Growth techniques are well established because of widespread in surface-acoustic-wave and timing applications, but unfortunately, it doesn't meet the birefringent phase matching condition due to small birefringence, and electric field poling condition due to lack of ferroelectricity. We devised a new poling technique in crystal quartz using mechanical twinning and demonstrated periodical polarity reversal by using thermal stress. Figure 1 shows an observed twin structure with a period of 80 μm, obtained by thermally induced stress between patterned Cr films and a quartz. The Cr patterned substrate was heated to just below Curie temperature in order to attain reasonable film stress and reduce coercive stress. Twins tend to generate from the edge of Cr pattern and the required duty ratio of Cr to the period was more than 0.5. The depth of twins, however, were several microns, indicating not suitable for bulk nonlinear optics. New technique is under development to improve the depth profile of the twins for a practical UV generator.

(a)

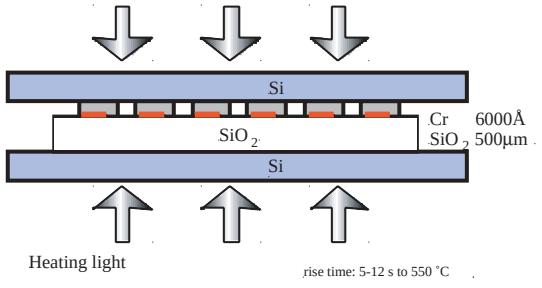

(b)

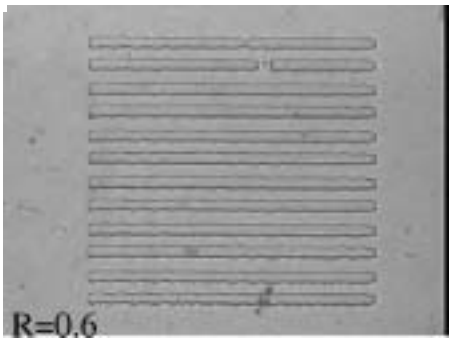

Figure 1. a) patterning method by the thermally induced in-plane stress b) observed periodical twins with a period of 80 μm period. R; duty ratio of the Cr film to the period.